journal

J. Am. Ceram. Soc., 94 [10] 3437–3441 (2011)
DOI: 10.1111/j.1551-2916.2011.04528.x

Synthesis, Characterization, and m-Xylene Sensing Properties of Co–ZnO Composite Nanofibers

Li Liu,[†,‡] Zhicheng Zhong,[§] Zhijun Wang,[‡] Lianyuan Wang,[‡] Shouchun Li,[‡] Zhen Liu,[‡] Yu Han,[‡] YunXia Tian,[‡] Peilin Wu,[§] and Xin Meng[§]

[‡]State Key Laboratory of Superhard Materials, College of Physics, Jilin University, Changchun 130012, China

[§]College of Instrumentation and Electrical Engineering, Jilin University, Changchun 130026, China

Co–ZnO composite nanofibers (0, 0.2, 0.4, and 0.8 wt%) are synthesized by electrospinning and calcination techniques. The fiber diameters are found to decrease by increasing the Co content in the ZnO nanofibers. The m-xylene sensing properties of the ZnO nanofibers are effectively enhanced with appropriate Co amount. The best sensing properties are found based on the 0.4 wt% Co–ZnO composite nanofibers at 320°C. The corresponding response is up to 14.8 when the sensor is exposed to 100 ppm m-xylene, and the response and recovery times are about 4 and 6 s, respectively. Moreover, excellent selectivity is also observed in the sensing investigation. The results make Co–ZnO composite nanofibers good candidates for fabricating high performance m-xylene sensors.

I. Introduction

THE ZnO is a chemically and thermally stable *n*-type II–VI compound semiconductor with a large band gap energy (3.37 eV at room temperature) and a strong exciton binding energy (60 meV).[1–3] It has been extensively studied for ultraviolet absorbers, optoelectronics, and field-emission devices, as well as gas sensors.[4–7] In the sensor field, ZnO has been proved to be a highly sensitive material for the detection of both reducing (e.g., CO, CH_4, and H_2) and oxidizing gases (e.g., Cl_2, O_2 and NO_x).[8–10] Recently, interest in one-dimensional (1D) ZnO nanostructures has been greatly stimulated because their sensing properties can be enhanced in this way.[11,12] In particular, the large surface-to-volume ratio of 1D nanostructures and the congruence of the carrier screening length with their lateral dimensions make them highly sensitive and efficient transducers of surface chemical processes into electrical signals.[11] Up to now, many promising sensing results based on 1D ZnO nanostructures have been reported. However, most of these investigations are focused on the ethanol, H_2, and CO sensing properties. The sensing results of the 1D ZnO nanostructures to organic gases have rarely been exposed.

Electrospinning is a unique technique which offers a relatively facile and versatile method for the large-scale synthesis 1D nanostructures that are exceptionally long in length, uniform in diameter, large in surface area, especially diversified in composition.[13] Our group has successfully synthesized several semiconductor nanofibers with different gas sensing properties by electrospinning.[14,15] In this paper, promoted by both the distinct properties of 1D nanostructure and the effects of metal additives on the sensing performance, we develop an *in situ* process for sensitizing ZnO by adding cobaltous nitrate during electrospinning and subsequent calcination. Gas sensing investigation exposes that this new type of nanofibers own improved and excellent m-xylene sensing properties at 320°C, which demonstrates that Co–ZnO composite nanofibers are very promising materials for fabricating practical m-xylene sensors.

II. Experimental Procedure

(1) Preparation and Characterization of Materials

Zinc nitrate, cobaltous nitrate, and poly(vinylpyrroridone) (PVP, $M_w = 1\,300\,000$) were supplied by Beijing Chemical Co. (Beijing, China). Ethanol and *N*,*N*-dimethylformamide (DMF) were bought from Tianjin Tiantai Chemical Co., (Tianjin, China). All the chemicals were analytical grade and used as received without further purification.

Co–ZnO composite nanofibers were synthesized by an electrospinning method and followed by calcination (Fig. 1).[16,17] In a typical procedure, 0.595 g of zinc nitrate and certain amount of cobaltous nitrate (0, 0.2 0.4, and 0.8 wt%) were added into a solvent of DMF in a glove box under vigorous stirring for 6 h. Subsequently, 1 g of PVP was dissolved into 8 mL ethanol in another glove box under vigorous stirring for 6 h. Then, both of them was mixed together under stirring and then loaded into a glass syringe for electrospinning by applying a high voltage of 18 kV at an electrode distance of 20 cm. The composite nanofibers were collected on an aluminum frame, transferred to a standard microscopic thin mica slide. After that, the organic constituents were selectively removed from these nanofibers by calcining them at 500°C for 5 h, and crystal nanofibers were obtained.

The crystal structures of the products were determined by X-ray powder diffraction (XRD) using an X-ray diffractometer (Siemens D5005, Munich, Germany). The morphologies of the electrospun nanofibers were viewed by scanning electron microscopy (SEM, SSX-550, Shimadzu equipped with energy dispersive X-ray (EDX) spectroscopy, Kyoto, Japan). Transmission electron microscopy (TEM, Model JEM-2000EX, JEOL, Tokyo, Japan) was performed with an accelerating voltage of 200 kV.

(2) Fabrication and Measurement of Sensors

The as-calcined sample was mixed with deionized water (resistivity = 18.0 MΩ/cm) in a weight ratio of 100:20 to form a paste. The paste was coated on a ceramic tube on which a pair of gold electrodes was printed previously, and then a Ni–Cr heating wire was inserted in the tube to form a side-heated gas sensor (Fig. 1).[18] The thickness of the sensing films was measured to be about 300 μm.

Gas sensing properties were measured by a CGS-8 (Chemical gas sensor-8) intelligent gas sensing analysis system (Beijing Elite Tech Co., Ltd., Beijing, China) (Fig. 1).[19] The sensors were

W. Mullins—contributing editor

Manuscript No. 28816. Received October 24, 2010; approved February 23, 2011.
This work was financially supported by the Department of Environmental Protection of Jilin Province (No. 2009-22), Jilin Provincial Science & Technology Department (No. 20100344), and the national innovation experiment program for university students (No. 2009C65125 and 2010C65188).
[†]Author to whom correspondence should be addressed. e-mail: liul99@jlu.edu.cn

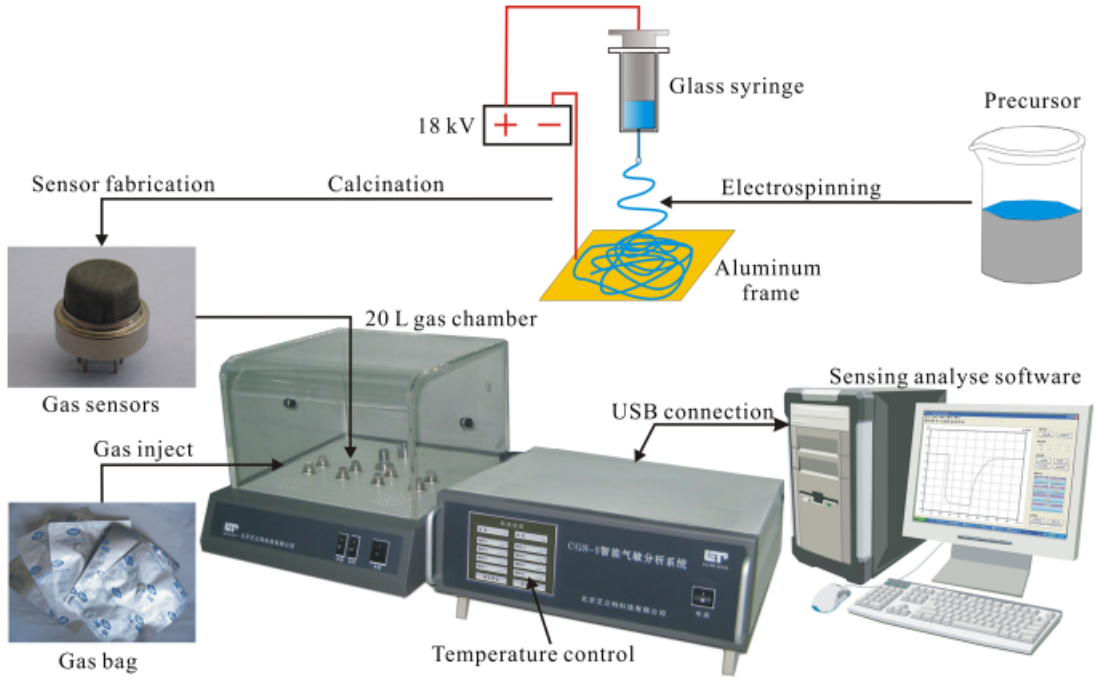

Fig. 1. Schematic diagram of the experimental apparatus.

preheated at different operating temperatures for about 30 min. When the resistances of all the sensors were stable, saturated target gas was injected into the test chamber (20 L in volume) by a micro-injector through a rubber plug. The saturated target gas was mixed with air (relative humidity was about 25%) by two fans in the analysis system. After the sensor resistances reached a new constant value, the test chamber was opened to recover the sensors in air. All the measurements were performed in a laboratory fume hood. The sensor resistance and response values were acquired by the analysis system automatically. The whole experiment process was performed in a super-clean room with the constant humidity and temperature (which were monitored by the analysis system).

The response value (R) was defined as $R = R_a/R_g$, where R_a was the sensor resistance in air (base resistance) and R_g was a mixture of target gas and air. The time taken by the sensor to achieve 90% of the total resistance change was defined as the response time in the case of response (target gas adsorption) or the recovery time in the case of recovery (target gas desorption).

III. Results and Discussion

Figure 2 shows the XRD patterns of 0, 0.2, 0.4, and 0.8 wt% Co–ZnO composite nanofibers. The samples are polycrystalline in nature. All the diffraction peaks can be indexed as hexagonal ZnO with lattice constants $a = 3.25$ Å and $c = 5.21$ Å, which are consistent with the values in the standard card (Joint Committee for Powder Diffraction Studies (JCPDS) card # 36-1451). For Co–ZnO composite nanofibers, the peak position of the wurtzite structure peaks shifts to higher angles compared with pure ZnO, but this tendency is not very obvious because of just a little difference ionic radius of Zn^{2+} (0.74 Å), Co^{2+} (0.74 Å), and Co^{3+} (0.63 Å) ions.

The EDX pattern of 0.4 wt% Co–ZnO composite nanofibers in Fig. 3 indicates that the as-prepared nanofibers are composed of ZnO, O, and Co. The patterns of 0.2 and 0.8 wt% Co–ZnO composite nanofibers are similar to the results in Fig. 3.

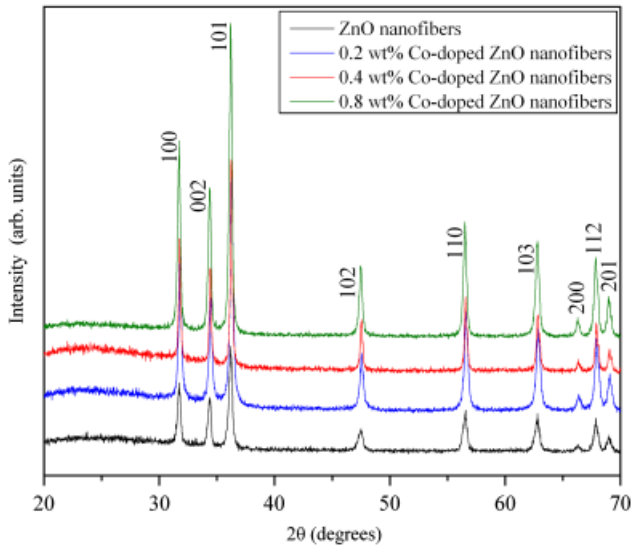

Fig. 2. X raydiffraction patterns of 0, 0.2, 0.4, and 0.8 wt% Co–ZnO composite nanofibers.

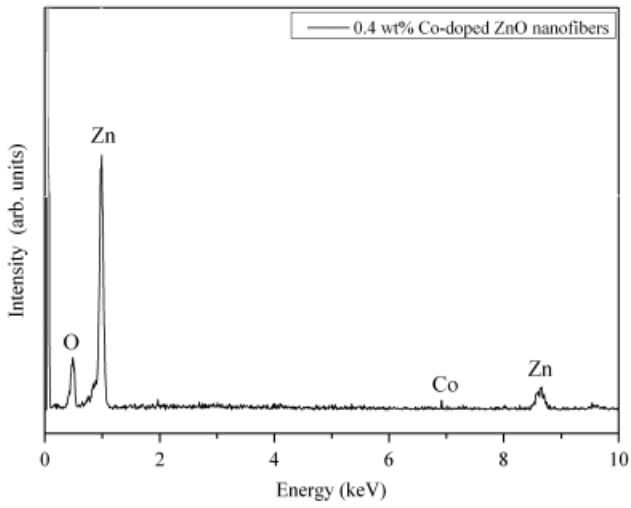

Fig. 3. Energy dispersive X-ray spectroscopyEDX pattern of 0.4 wt% Co–ZnO composite nanofibers.

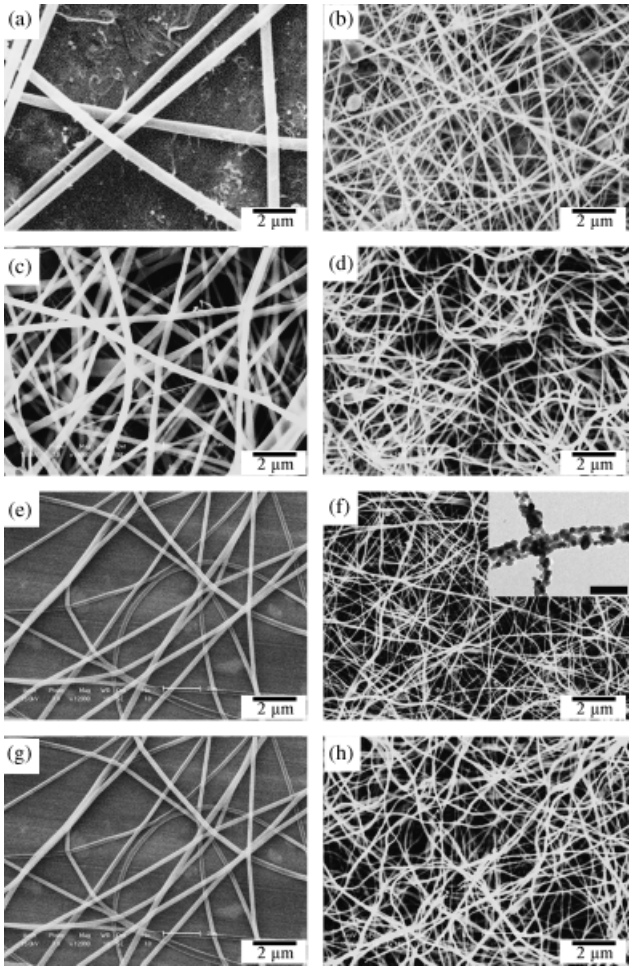

Fig. 4. Scanning electron microscopic images of precursors ((a) 0, (c) 2 wt%, (e) 4 wt%, and (g) 8 wt%) and calcinated products ((b) 0, (d) 2 wt%, (f) 4 wt%, and (h) 8 wt%) of Co–ZnO composite nanofibers. The inset in (f) shows a corresponding TEM image, and the scale bar is 200 nm.

The morphologies on the precursors (zinc nitrate/cobaltous nitrate/PVP composite fibers) tuned by different amounts of cobaltous nitrate, with other conditions fixed, have been measured by SEM as shown in Figs. 4(a), (c), (e), and (g), respectively. From these SEM images, it can be clearly seen that the diameters of the precursors become thinner by increasing the amounts of cobaltous nitrate. The average diameters of the 0, 2, 4, and 8 wt% Co–ZnO composite nanofibers are about 180, 160, 130, and 130 nm, respectively. This is because the charges (Co^{2+}, Co^{3+}, and NO_3^-) added during the electrospinning will make the fibers thinner.[20] After calcination, the diameters of the products, as shown in Figs. 4(b), (d), (f), and (h), are thinner than those of the precursors, indicating the removal of PVP template.

Gas sensing experiments were performed at different temperatures to find out the optimum operating condition for m-xylene detection. Figure 5 shows the responses of 0, 0.2, 0.4, and 0.8 wt% Co–ZnO composite nanofibers to 100 ppm m-xylene at different operating temperatures. The responses of all samples are found to increase with increasing the operating temperature, which attain their maximum, and then decrease with a further rise of the operating temperature. This behavior can be explained from the kinetics and mechanics of gas adsorption and desorption on the surface of ZnO or similar semiconducting metal oxides.[21–23] When the operating temperature is too low, the active of nanofibers is consequently small, leading to a very small response. When the operating temperature increased too much, some observed gas molecules may escape before their reaction due to their high active, thus the response will decrease

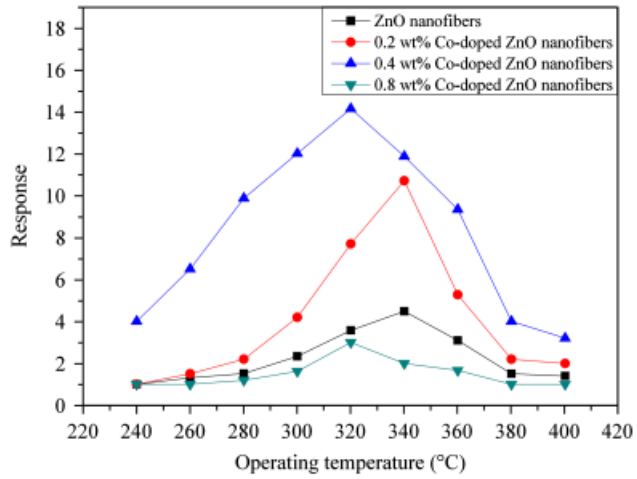

Fig. 5. Responses of 0, 0.2, 0.4, and 0.8 wt% Co–ZnO composite nanofibers to 100 ppm m-xylene at different temperatures.

correspondingly. Furthermore, it can be found that Co adding can decrease the optimal operating temperature (corresponding to the maximum response value) of ZnO nanofibers to m-xylene. The optimal operating temperatures of 0% and 0.2 wt% Co–ZnO composite nanofibers are about 340°C, and are about 320°C for 0.4 and 0.8 wt% composite samples. This behavior suggests that Co may decrease the reaction energy between m-xylene and oxygen species on ZnO nanofibers.[24] The maximum response (about 14.8) among all the samples is found based on the 0.4 wt% Co–ZnO composite nanofibers at 320°C, which is 3.4 times larger than that of pure ZnO nanofibers at 320°C (about 4.4). Thus this composite sample is applied in all the investigations hereinafter. The base resistances (R_a) of the sensors based on 0, 0.2, 0.4, and 0.8 wt% Co–ZnO composite nanofibers are about 1.3, 1.4, 1.8, and 10.7 MΩ, respectively.

Figure 6 shows the responses of 0 and 0.4 wt% Co–ZnO composite nanofibers to different concentrations of m-xylene at 320°C. Adding Co in ZnO nanofibers can effectively improve their m-xylene sensing properties. The responses of pure ZnO nanofibers are about 1.3, 4.5, 7, 14, and 20 to 2, 50, 100, 500, and 1000 ppm m-xylene, and are about 3, 11, 14.8, 37, and 52 for Co–ZnO composite nanofibers, respectively.

The 0.4 wt% Co–ZnO composite nanofibers also exhibit rapid response/recovery characteristics to m-xylene at 320°C, as shown in Fig. 7. The response and recovery times are about 4 and 6 s, respectively. Such rapid response is based on the structures of as-prepared fibers. The large surface of the ZnO nanofibers makes the absorption of m-xylene molecules on the

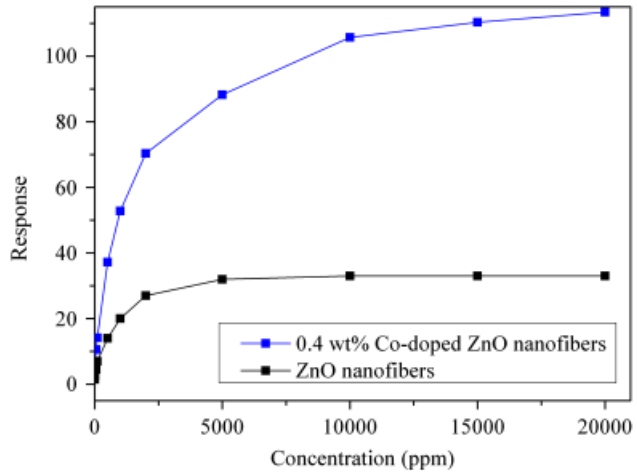

Fig. 6. Responses of 0 and 0.4 wt% Co–ZnO composite nanofibers to different concentrations of m-xylene at 320°C.

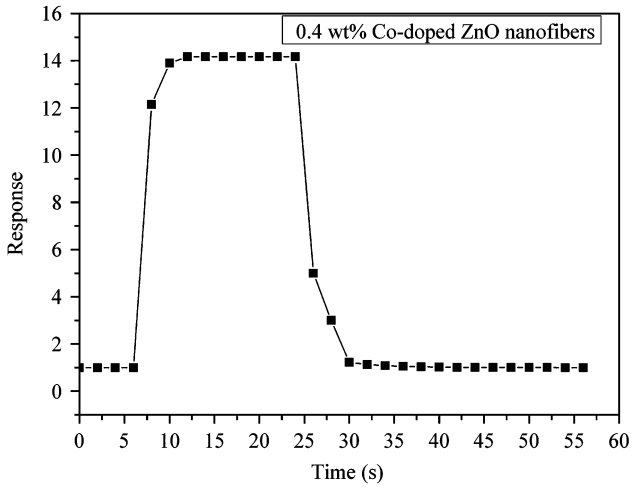

Fig. 7. Response and recovery characteristics of 0.4 wt% Co–ZnO composite nanofibers to 100 ppm m-xylene at 320°C.

surface of the material easily. The 1D structures of the fibers can facilitate fast mass transfer of the m-xylene molecules to and from the interaction region as well as improve the rate for charge carriers to transverse the barriers induced by molecular recognition along the fibers. On the other hand, comparing with 2D nanoscale films, the interfacial areas between the active sensing region of the nanofibers and the underlying substrate is great reduced.[11,12] Additionally, Co may also accelerate the reaction between ZnO nanofibers and m-xylene gas molecules.[25] Those advantages lead to the significant gain in the fast response and recovery of the as-prepared sensors.

The 0.4 wt% Co–ZnO composite nanofibers exhibit excellent selectivity at 320°C, as shown in Fig. 8. The response of Co–ZnO composite nanofibers to100 ppm m-xylene ($C_6H_5(CH_3)_2$) is more than 3 times larger than that to toluene ($C_6H_5CH_3$), benzene (C_6H_6), and ethanol (C_2H_5OH). Usually, chemical sensors fabricated from metal oxides cannot distinguish these common interference gases. The excellent selectivity in this case is based on the optimizing operating temperatures of Co–ZnO composite nanofibers to various target gases are different.[26] As can be seen in Fig. 8, Co–ZnO composite nanofibers show more sensitive to C_2H_5OH than to m-xylene at 360°C, and they also show higher response to toluene than to m-xylene at 380°C.

The sensing mechanism can be explained as follows.[27–29] When the ZnO nanofibers are surrounded by air, oxygen molecules will adsorb on the fiber surface to generate chemisorbed oxygen species (O is believed to be dominant),[27] and resulting in

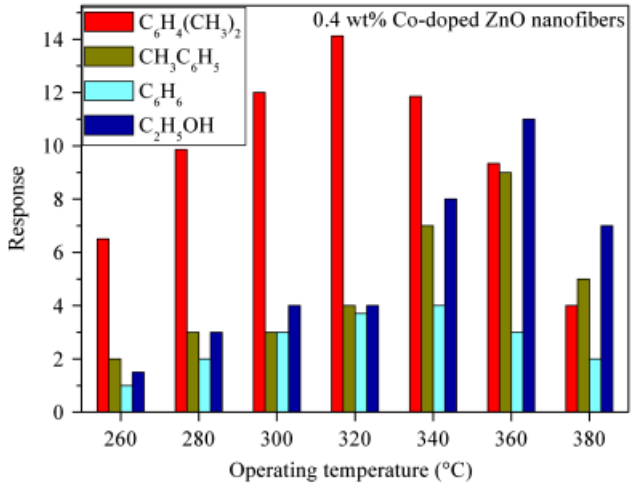

Fig. 8. Responses of 0.4 wt% Co–ZnO composite nanofibers to 100 ppm different gases at different operating temperatures.

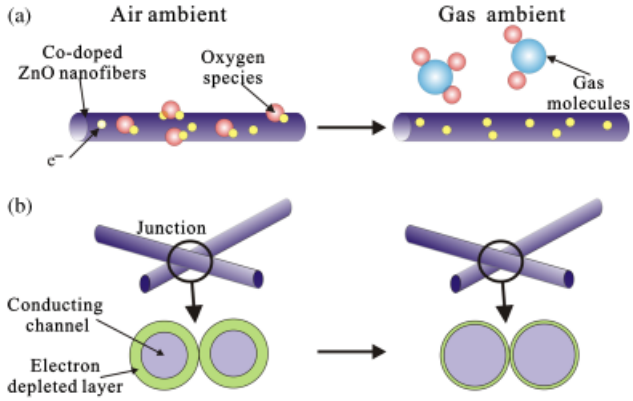

Fig. 9. Schematic diagram of ZnO nanofiber sensing mechanism.

a high resistance. When m-xylene is introduced at a moderate temperature (the optimizing operating temperature), these nanofibers are exposed to the traces of reductive gas. By reacting with the oxygen species on the ZnO surface, the reductive m-xylene will reduce the concentration of oxygen species on the ZnO surface and thus increase the conductivity of ZnO nanofibers. The reaction between surface oxygen species and m-xylene can be simply described as follows (Fig. 9(a)):

$$O_2\,(\text{gas}) \longleftrightarrow O_2\,(\text{ads}) \quad (1)$$

$$O_2\,(\text{ads}) + e^- \longleftrightarrow O_2^-\,(\text{ads}) \quad (2)$$

$$O_2^-\,(\text{ads}) + e^- \longleftrightarrow 2O^-\,(\text{ads}) \quad (3)$$

$$O^-\,(\text{ads}) + e^- \longleftrightarrow O^{2-}\,(\text{ads}) \quad (4)$$

$$2C_6H_5(CH_3)_2 + 43O^- \longleftrightarrow 16CO_2 + 11H_2O + 43e^- \quad (5)$$

The good sensing properties such as high response and short response/recovery times of Co–ZnO composite nanofibers are mainly based on the fiber structure combing with the Co adding. The 1D nanostructure of ZnO nanofibers possesses large surface-to-volume ratio, which can absorb more target gas molecules on the fiber surface.[11] And the Co–ZnO composite nanofibers synthesized by electrospinning own high length-to-diameter ratio (can be found in SEM images), which may form netlike structure on the sensor surface.[30] This netlike structure will further enhance the gas adsorption, and lead to a high response value. Besides, there are many nanofiber–nanofiber junctions in the netlike structure (Fig. 9(b)). Such junctions should form a depleted layer around the intersection and block the electron flow in a way which is more efficient than the surface depletion on the individual nanofibers (contact-controlled effect).[31] Moreover, the high sensing properties of these nanofibers are also related to the decreased and uniform fiber diameter, as shown in (Fig. 4).[11,30]

Many former papers have proved that the existence of Co in semiconductor sensing materials can improve their response prominently.[25,32–34] In this case, decreased fiber diameter caused by Co adding will lead to an increase of target gas adsorption (shown in Fig. 4), and resulted in the sensing improvement. On the other hand, Co supports the catalytic conversion of m-xylene into its oxidation products, which is due to spill-over of activated fragments to the semiconductor surface to react with the adsorbed oxygen and is called chemical sensitization. And this effect can accelerate the sensing reaction on the fiber surface effectively.[12] Moreover, as Co_3O_4 is a *p*-type material,[32–34] adding too much Co in ZnO may form Co_3O_4 (although not found in XRD pattern due to its very small amount) in ZnO nanofibers and the *n*-type characteristics of the ZnO will regress (corresponding to an evident increase in R_a), thus the sample with 0.8 wt% composite rate shows a decreased response.

IV. Conclusions

In summary, Co–ZnO composite nanofibers with different composite rates are synthesized by electrospinning and calcination techniques, and their gas sensing properties are investigated. Co–ZnO composite nanofibers exhibit high response, short response/recovery times, and excellent selectivity to m-xylene. The sensing mechanism is discussed based on the fiber structure and Co adding effect.

References

[1]Y. Qiu and S. Yang, "ZnO Nanotetrapods: Controlled Vapor-Phase Synthesis and Application for Humidity Sensing," *Adv. Funct. Mater.*, **17**, 1345–52 (2007).

[2]B. Liu and H. C. Zeng, "Hydrothermal Synthesis of ZnO Nanorods in the Diameter Regime of 50 nm," *J. Am. Chem. Soc.*, **125**, 4430–1 (2003).

[3]Z. W. Pan, Z. R. Dai, and Z. L. Wang, "Nanobelts of Semiconducting Oxides," *Science*, **291**, 1947–9 (2001).

[4]L. A. Patil, A. R. Bari, M. D. Shinde, and V. Deo, "Ultrasonically Prepared Nanocrystalline ZnO Thin Films for Highly Sensitive LPG Sensing," *Sens. Actuators B Chem.*, **149**, 79–86 (2010).

[5]V. Kobrinsky, E. Fradkin, V. Lumelsky, A. Rothschild, Y. Komem, and Y. Lifshitz, "Tunable Gas Sensing Properties of *p*- and *n*-Doped ZnO Thin Films," *Sens. Actuators B Chem.*, **148**, 379–87 (2010).

[6]J. Singh, S. S. Patil, M. A. More, D. S. Joag, R. S. Tiwari, and O. N. Srivastava, "Formation of Aligned ZnO Nanorods on Self-Grown ZnO Template and Its Enhanced Field Emission Characteristics," *Appl. Surf. Sci.*, **256**, 6157–63 (2010).

[7]F. Boccuzzi, A. Chiorino, S. Tsubota, and M. Haruta, "An IR Study of CO-Sensing Mechanism on Au/ZnO," *Sens. Actuators B Chem.*, **24–25**, 540–3 (1995).

[8]Z. P. Sun, L. Liu, L. Zhang, and D. Z. Jia, "Rapid Synthesis of ZnO Nano-Rods by One-Step, Room-Temperature, Solid-State Reaction and Their Gas-Sensing Properties," *Nanotechnology*, **17**, 2266–70 (2006).

[9]Q. Qi, T. Zhang, S. Wang, and X. Zheng, "Humidity Sensing Properties of KCl-Doped ZnO Nanofibers with Super-Rapid Response and Recovery," *Sens. Actuators B Chem.*, **137**, 649–55 (2009).

[10]W. Z. Xu, Z. Z. Ye, D. W. Ma, H. M. Lu, L. P. Zhu, B. H. Zhao, X. D. Yang, and Z. Y. Xu, "Quasi-Aligned ZnO Nanotubes Grown on Si Substrates," *Appl. Phys. Lett.*, **87**, 093110, 3pp (2005).

[11]A. Kolmakov and M. Moskovits, "Chemical Sensing and Catalysis by One-Dimensional Metal-Oxide Nanostructures," *Annu. Rev. Mater. Res.*, **34**, 151–80 (2004).

[12]M. E. Franke, T. J. Koplin, and U. Simon, "Metal and Metal Oxide Nanoparticles in Chemiresistors: Does the Nanoscale Matter," *Small*, **2**, 36–50 (2006).

[13]A. Greiner and J. H. Wendorff, "Electrospinning: A Fascinating Method for the Preparation of Ultrathin Fibers," *Angew. Chem. Int. Ed.*, **46**, 5670–703 (2007).

[14]L. Liu, T. Zhang, Z. J. Wang, S. C. Li, Y. X. Tian, and W. Li, "High Performance Micro-Structure Sensor Based on TiO_2 Nanofibers for Ethanol Detection," *Chin. Phys. Lett.*, **26**, 090701, 4pp (2009).

[15]L. Liu, S. Li, J. Zhuang, C. Guo, L. Wang, and W. Li, "Enhancement of Ethanol Sensing Properties of Ni-Doped SnO_2 Nanofibers," *J. Am. Ceram. Soc.*, (in press).

[16]X. F. Song, Z. J. Wang, Y. B. Liu, C. Wang, and L. J. Li, "A Highly Sensitive Ethanol Sensor Based on Mesoporous ZnO–SnO_2 Nanofibers," *Nanotechnology*, **20**, 075501–5 (2009).

[17]Z. J. Wang, Z. Y. Li, L. Liu, X. R. Xu, H. N. Zhang, W. Wang, W. Zheng, and C. Wang, "A Novel Alcohol Detector Based on ZrO_2-Doped SnO_2 Electrospun Nanofibers," *J. Am. Ceram. Soc.*, **93**, 634–7 (2010).

[18]Q. Qi, T. Zhang, X. Zheng, H. Fan, L. Liu, R. Wang, and Y. Zeng, "Electrical Response of Sm_2O_3-Doped SnO_2 to C_2H_2 and Effect of Humidity Interference," *Sens. Actuators B Chem.*, **134**, 36–42 (2008).

[19]H. Zhang, Z. Li, L. Liu, X Xu, Z. Wang, W. Wang, W. Zheng, B. Dong, and C. Wang, "Enhancement of Hydrogen Monitoring Properties Based on Pd–SnO_2 Composite Nanofibers," *Sens. Actuators B Chem.*, **147**, 111–5 (2010).

[20]H. Hou, Z. Jun, A. Reuning, A. Schaper, J. H. Wendorff, and A. Greiner, "Poly (*p*-xylylene) Nanotubes by Coating and Removal of Ultrathin Polymer Template Fibers," *Macromolecules*, **35**, 2429–31 (2002).

[21]N. Yamazoe, J. Fuchigami, M. Kishikawa, and T. Seiyama, "Interactions of Tin Oxide Surface with O_2, H_2O and H_2," *Surf. Sci.*, **86**, 335–44 (1979).

[22]J. Herrán, O. Fernández-González, I. Castro-Hurtado, T. Romero, G. G. Mandayo, and E. Castaño, "Photoactivated Solid-State Gas Sensor for Carbon Dioxide Detection at Room Temperature," *Sens. Actuators B Chem.*, **149**, 368–72 (2010).

[23]M. Ghasdi and H. Alamdari, "CO Sensitive Nanocrystalline $LaCoO_3$ Perovskite Sensor Prepared by High Energy Ball Milling," *Sens. Actuators B Chem.*, **148**, 478–85 (2010).

[24]S. Shukla, P. Zhang, H. J. Cho, S. Seal, and L. Ludwing, "Room Temperature Hydrogen Response Kinetics of Nano-Micro-Integrated Doped Tin Oxide Sensor," *Sens. Actuators B Chem.*, **120**, 573–83 (2007).

[25]K. I. Choi, H. R. Kim, K. M. Kim, D. Liu, G. Cao, and J. H. Lee, "C_2H_5OH Sensing Characteristics of Various Co_3O_4 Nanostructures Prepared by Solvothermal Reaction," *Sens. Actuators B Chem.*, **146**, 40–5 (2010).

[26]Q. Qi, T. Zhang, L. Liu, X. Zheng, Q. Yu, Y. Zeng, and H. Yang, "Selective Acetone Sensor Based on Dumbbell-Like ZnO with Rapid Response and Recovery," *Sens. Actuators B Chem.*, **134**, 166–70 (2008).

[27]Y. Shimizu, S. Kai, Y. Takao, T. Hyodo, and M. Egashira, "Correlation Between Methylmercaptan Gas-Sensing Properties and Its Surface Chemistry of SnO_2-Based Sensor Materials," *Sens. Actuators B Chem.*, **65**, 349–57 (2000).

[28]M. Egashira, N. Kanehara, Y. Shimizu, and H. Iwanaga, "Gas-Sensing Characteristics of Li^+-Doped and Undoped ZnO Whiskers," *Sens. Actuators B Chem.*, **18**, 349–60 (1989).

[29]N. Barsan, D. Koziej, and U. Weimar, "Metal Oxide-Based Gas Sensor Research: How to?," *Sens. Actuators B Chem.*, **121**, 18–35 (2007).

[30]Y. Zhang, J. Li, G. An, and X. He, "Highly Porous SnO_2 Fibers by Electrospinning and Oxygen Plasma Etching and Its Ethanol-Sensing Properties," *Sens. Actuators B Chem.*, **144**, 43–8 (2010).

[31]P. Feng, Q. Wan, and T. H. Wang, "Contact-Controlled Sensing Properties of Flowerlike ZnO Nanostructures," *Appl. Phys. Lett.*, **87**, 213111, 3pp (2005).

[32]R. J. Wu, J. G. Wu, M. R. Yu, T. K. Tsai, and C. T. Yeh, "Promotive Effect of CNT on Co_3O_4–SnO_2 in a Semiconductor-Type CO Sensor Working at Room Temperature," *Sens. Actuators B Chem.*, **131**, 306–12 (2008).

[33]T. Xu, H. Huang, W. Luan, Y. Qi, and S. Tu, "Thermoelectric Carbon Monoxide Sensor Using Co–Ce Catalyst," *Sens. Actuators B Chem.*, **133**, 70–7 (2008).

[34]M. Siemons and U. Simon, "Preparation and Gas Sensing Properties of Nanocrystalline La-Doped $CoTiO_3$," *Sens. Actuators B Chem.*, **120**, 110–8 (2006). □